NOx storage and reduction properties of Pt/CexZr1–xO2 mixed oxides: Sulfur resistance and regeneration, and ammonia formation

N. Le Phuc, E.C. Corbos, Xavier Courtois, F. Can, P. Marecot, D. Duprez

Applied Catalysis B: Environmental 93 (2009) 12–21.
DOI: 10.1016/j.apcatb.2009.09.007

NOx storage and reduction properties of $Pt/Ce_xZr_{1-x}O_2$ mixed oxides: sulfur resistance and regeneration, and ammonia formation.

N. Le Phuc, E.C. Corbos, X. Courtois*, F. Can, P. Marecot, D. Duprez
Laboratoire de Catalyse en Chimie Organique, Université de Poitiers, UMR6503 CNRS,
40 Av. Recteur Pineau, Poitiers, 86022, France
*Corresponding author: E-mail: xavier.courtois@univ-poitiers.fr

Abstract

The influence of the ceria-zirconia mixed oxide composition in $Pt/Ce_xZr_{1-x}O_2$ catalysts was studied toward NOx storage capacity, including sulfur poisoning and sulfur regeneration, and NOx reduction efficiency in lean-rich cycling conditions. The results are compared with a Pt/Ba/Al model catalyst. The samples were characterized by N_2 adsorption, XRD and H_2-TPR. The behaviors of the ceria-zirconia supported catalysts are quite similar whatever their composition. They are sensitive to a reducing pre-treatment which lead to an increase of (i) the cerium reducibility/oxygen mobility, (ii) the NO oxidation rate and (iii) the NOx storage capacity at 300 and 400°C. The sulfating treatment leads to a dramatic decrease of the NOx storage capacity for all catalysts, the decrease being more pronounced for the Zr-rich samples. H_2-TPR experiments show that the sulfates amount and their stability tend to increase with the Zr content, but these sulfates are significantly less stable compared with Pt/Ba/Al. The sulfur elimination rates in rich mixture at 550°C are higher than 90% with the ceria-zirconia supported catalysts versus 56% with Pt/Ba/Al.
The ceria-zirconia supported catalysts are able to convert NOx in lean-rich cycling condition. Compared with Pt/Ba/Al, the NOx conversions are a little lowered but the ammonia selectivity is significantly decreased with the Ce-Zr mixed oxides, with a beneficial influence of the cerium content.

Keywords: NOx, storage, reduction, ceria, zirconia, ammonia formation

1. Introduction:

The general demand for lower CO_2 emissions leads to the development of diesel and lean-burn engines. Exhaust gases from these engines contain NO_x in excess of O_2, which makes NO_x reduction into N_2 very difficult. One possible way to reduce NOx emissions is to use a NOx storage reduction (NSR) catalyst [1]. It works mainly in lean condition, and the NOx are then oxidized on the precious metals and stored on basic compounds, mainly as nitrates. Periodically, the system switches to rich conditions for few seconds, and the nitrates previously formed during the first step are reduced into N_2 on the precious metals [2,3]. The most investigated systems are Pt based catalysts supported on alumina and barium oxide is added as NOx storage material. One of the disadvantages of this catalyst is the deactivation, mainly due to sulfur poisoning and to thermal aging.

Sulfur poisoning [4] is coming from the combustion of sulfur molecules present in fuels and oils, leading to SO_2 in the exhaust gas. In oxidizing atmosphere SO_2 is oxidized into SO_3 which is trapped as sulfate on the NOx storage sites. Unfortunately, the sulfates are more strongly adsorbed than the corresponding nitrates. Then, the regeneration of a poisoned catalyst needs high temperature in rich atmosphere [5], inducing an overconsumption. Moreover, very stable barium sulfate can be formed under oxidizing atmosphere at high temperature, with formation of bulk sulfate [5].

High temperatures not only lead to sulfate stabilization when barium is poisoned, but also to sintering of the precious metals and storage material. For barium/alumina catalysts, formation of $BaAl_2O_4$ (spinel structure) is also observed [6].

Numerous studies were focused on the storage material in order to improve the NOx storage catalysts. For instance, Huang et al. have shown a good sulfur resistance of a $Pt\text{-}Rh/TiO_2/Al_2O_3$ catalyst [7]. However, barium is the most commonly used storage material and some sulfur tolerance was obtained by addition of other oxides. Yamazaki et al. have studied the impact of Fe, Co, Ni and Cu addition. They have observed the best beneficial effect with the iron addition which was attributed to inhibition of the bulk $BaSO_4$ formation [8]. Tin addition to barium in order to form a $BaSnO_3$ perovskites can also lead to a sulfur tolerance for low temperature applications (100-300°C) [9]. More recently, it has been demonstrated that a Mg-Ba storage material exhibits a high resistance to deactivation by SO_2 [10]. However, the roles of cerium compounds, which are largely used in automotive catalysts, are not extensively studied yet in NSR system. They are thought to intervene in the different steps of the NOx trap process: NO oxidation, NOx storage; and NOx reduction. The cerium compounds probably accelerate the hydrocarbon partial oxidation during rich-spikes (giving CO and H_2 as NOx reducers). This beneficial effect competes with the reduction of the materials itself due to its oxygen storage capacity (OSC), that may delay HC decomposition and thus NOx reduction [1]. However, some results show that cerium compounds in NOx-trap system can lead to interesting properties. First, they improve the barium stability. Eberhardt et al. [11] have compared the behavior of Ba/Al_2O_3 and Ba/CeO_2 materials. No solid/solid reaction between Ba and ceria was observed below 780°C under air, while Ba reacted at lower temperature with Al_2O_3 to form inactive barium aluminates. These results are not totally in accordance with those of Casapu et al. [12]. They have shown that the barium cerate formation is easier than the barium aluminates formation, but they also demonstrated that $BaCeO_3$ is easily decomposed under $NO_2\text{-}H_2O$ (300-500°C temperature range) and destabilized under CO_2, whereas $BaAl_2O_4$ is stable. Liotta et al.

[13] have also observed interaction between cerium and barium compounds in a Pt-CeZrOx/Ba-Al_2O_3 NOx-trap catalyst, with a migration of Ba ions through the CeZrOx compound. This Ba-Ce interaction could allow a better control of the Ba dispersion as well as an improvement of the resistance to SO_2 poisoning [14]. Furthermore, it was also previously established that ceria compounds are able to store NOx. The NO/O_2 adsorption on pure ceria was studied by Philipp et al. [15] and the cerium-based compounds participation for the NO storage was putted in evidence in several studies [13,16]. For example, Ba/CeO_2 material has exhibited a higher NOx storage efficiency than Ba/Al_2O_3 within the temperature range of 200-400°C [11]. Similar results were obtained by Lin et al. [17] who investigated the effect of La or Ce addition on the NOx storage properties of $Pt/Ba\text{-}Al_2O_3$. Substituting La for Ce increased the NOx storage capacity from 341 µmol g^{-1} in $Pt_{2.5}La_{30.5}Ba_{33.4}Al_{100}$ to 1020 µmol g^{-1} for the $Pt_{2.5}Ce_{30.5}Ba_{33.4}Al_{100}$ catalyst. Nakatsuji et al. [18] have studied the effect of cerium-based materials on rhodium catalysts deposited on Ce, Ce-Zr, Ce-Pr, Ce-Nd-Pr and Ce-Gd-Zr oxides. Compared to Al_2O_3, ZrO_2 or beta zeolite, these catalysts allow a high DeNOx activity under lean-rich (55s-5s) cycling condition, even in large O_2 excess during the lean period.
It is important to note that the optimal storage temperature is depending on the storage material. In a previous study, we have compared the NOx storage capacities of $Pt/Ce_{0.7}Zr_{0.3}O_2$ with a usual $Pt/Ba/Al_2O_3$ model catalyst and with $Pt/Ba/Ce_{0.7}Zr_{0.3}O_2$. At low temperature (200°C), $Pt/Ce_{0.7}Zr_{0.3}O_2$ exhibited the higher NOx storage capacity, whereas at 400°C the best capacity was obtained with $Pt/Ba/Ce_{0.7}Zr_{0.3}O_2$ [19]. These results were attributed to different basicity and inducing different competition between NOx, CO_2 and H_2O. The low temperature efficiency of ceria based storage material was also demonstrated with $MnO_x\text{-}CeO_2$ oxide [20].
These ceria containing catalysts also exhibited very interesting properties especially toward regeneration after sulfating, because the cerium sulfates are less stable than barium sulfates [14,19,21].
Numerous ceria-zirconia compositions are used in automotive catalyst. They are well known for their oxygen storage capacity and their thermal resistance to sintering compared to pure ceria. However, to our knowledge, the impact of the ceria-zirconia composition on the NOx trap behavior was not investigated yet. In the present work, we have studied the NOx storage capacity, the sulfur resistance and regeneration and the NOx removal efficiency of $Pt/Ce_xZr_{1-x}O_2$ oxides with x = 1; 0.70; 0.58; 0.20. The results are compared to a $Pt/10\%BaO/Al_2O_3$ model NSR catalyst. Note that the 10% BaO may be not the optimal loading but it allows determining if the DeNOx properties of the ceria-zirconia materials are in the same order of magnitude or not. In fact, numerous studies have been performed on the Ba loading, generally included between 5-30 wt%, that shown that the Ba content influenced the Pt–Ba proximity, the Ba dispersion and the surface basicity of the catalysts [22,23]. One of the most studied catalysts remains Pt/Ba/Al, which can be used as material of reference.

2. Experimental:

2.1. Catalysts preparation

A CeO_2 oxide and three $Ce_xZr_{1-x}O_2$ solid solutions (x = 0.70; 0.58; 0.20), all provided by Rhodia, were used in this work as catalyst support. They were first calcined 4 hours under air at 700°C before use. Platinum was then impregnated with a $Pt(NH_3)_2(NO_2)_2$ solution in order

to have 1wt%Pt content. After drying and calcinations under air at 450°C, the samples were stabilized 4 hours at 700°C under a O_2, H_2O, N_2 mixture. The catalysts are noted Pt/CeX (X=100, 70, 58, 20) depending on the ceria content in the support, i.e. for x = 1; 0.70; 0.58; 0.20 in $Ce_xZr_{1-x}O_2$, respectively.

A reference 1wt%Pt/10wt%BaO/Al_2O_3 catalyst was prepared by impregnation of an alumina support with a barium nitrate solution. After calcination of the support at 700°C under air, platinum was impregnated with a $Pt(NH_3)_2(NO_2)_2$ solution. The sample was then dried, calcined and stabilized as described above. It is denoted Pt/Ba/Al.

To study the impact of a reducing pre-treatment, the catalysts were submitted to pure hydrogen 4 hours at 700°C and cooled under N_2 until room temperature before exposure to air. These reduced catalysts are denoted R700.

The catalysts were sulfated by exposure to a 100ppm SO_2, 10% O_2, 10% H_2O and N_2 mixture at 400°C for 5h. The quantity of SO_2 introduced during the sulfating treatment corresponds to a 2.0 wt % S content if all the sulfur is stored on the catalyst. These sulfated catalysts are denoted +S.

The regeneration of the sulfated catalysts was performed under reducing condition with 2.5% H_2, 10% CO_2, 10% H_2O and N_2. The catalyst is heated under this mixture from room temperature up to the regeneration temperature (450, 500 or 550°C, heating rate: 10°C.min^{-1}) and maintained at this temperature for 30 min before cooling under N_2. The regenerated catalysts are denoted +R450, +R500 or +R550, respectively.

Some aging were also performed before or after the sulfating treatment. The sample was submitted to a mixture containing 10% O_2, 10% CO_2, 10% H_2O and N_2 at 800°C for 30 min. The corresponding samples are named +A800.

2.2. NOx storage capacity (NSC) measurement

Before the NOx storage capacity measurements, the catalyst (60mg) was pretreated *in situ* for 30 min at 550°C (or 300°C for the sulfated samples), under a 10% O_2, 10% H_2O, 10% CO_2 and N_2 mixture (total flow rate: 10 L.h^{-1}), and then cooled down to the storage temperature under the same mixture. The sample was then submitted to 350ppm NO, 10% O_2, 10% H_2O, 10% CO_2 and N_2 (total flow rate: 10 L.h^{-1}) at 200°C, 300°C and 400°C. The gas flow was introduced using mass-flow controllers, except for H_2O which was introduced using a saturator. Both NO and NOx concentrations ($NO+NO_2$) were followed by chemiluminescence. H_2O was removed prior to NOx analysis with a membrane dryer. Long time storage is not representative of the NSR catalyst working conditions, since the lean periods are commonly around 1 min. The NOx storage capacity was then estimated by the integration of the recorded profile for the first 100 seconds to minimize the uncertainty due to the subtraction of the reactor volume contribution. With the conditions used in this test, 67µmol NOx per gram of catalyst are injected in 100s. In addition, the platinum oxidation activity was estimated as the NO_2/NOx ratio (%) at saturation (usually about 900s).

2.3. NOx conversion in cycling conditions

Before measurement, the catalyst (100mg) was treated *in situ* at 550°C under 10% O_2, 10% H_2O, 10% CO_2 and N_2. The sample was then cooled down to test temperatures (200, 300 and 400°C) under the same mixture. The NOx conversion was studied in cycling condition by

alternatively switching between lean (30s) and rich (10s) conditions using electro-valves. These relatively short lean periods were used to have better evidence of the different behaviors. The gas composition is described in Table 1. NO and NO_2 were followed by chemiluminescence, N_2O by specific FTIR, H_2 by mass spectrometry. Before the analyzers, H_2O was removed in a condenser at 0°C. For each studied temperature, the activity of the catalysts was followed until stabilization. After stabilization, the outlet water was condensed for one hour in a dry condenser and then analyzed by two different HPLC for NH_4^+, NO_2^- and NO_3^-. NO_2^- and NO_3^- were added to the unconverted NOx. The N_2 selectivity is calculated assuming no other N-compounds than NO, NO_2, N_2O, NH_3. Some tests were also performed using a Multigas FTIR detector (MKS 2030) without water trap system.

Table 1: NOx removal efficiency test: gas composition for the lean and rich mixtures. Total flow rate: 167 $ml.min^{-1}$.

Gas	NO	O_2	H_2	CO_2	H_2O	N_2
Lean (30s)	500 ppm	10 %	-	10 %	10 %	Balance
Rich (10s)	-	-	3 or 6 %	10 %	10 %	Balance

2.4. Temperature programmed reduction (TPR)

Prior to the TPR test, the catalyst (50 mg) was first pretreated *in situ* under oxygen at 300°C for 30 min and cooled to room temperature. After flushing under argon for 45 min, the reduction was carried out from room temperature up to 800°C under a 1%H_2/Ar mixture, using a 5°C min^{-1} heating rate. The sample was maintained at 800°C for 30 min before cooling under argon. Hydrogen consumption was followed by thermal conductivity.

2.5. X-ray diffraction

X-ray powder diffraction was performed at room temperature with a Bruker D5005 using a Kα Cu radiation (λ=1.54056 Å). The powder was deposited on a silicon monocrystal sample holder. The crystalline phases were identified by comparison to the ICDD database files.

2.6. Specific surface measurement

The BET surface areas were deduced from N_2 adsorption at -196°C carried out with a Micromeritics apparatus. Prior to the measurement, the samples were treated at 250°C under vacuum for 8 h to eliminate the adsorbed species.

2.7. Oxygen storage capacity (OSC)

The OSC was measured at 200, 300 400°C under atmospheric pressure. The sample (5 mg) was continuously purged with helium (30 $mL.min^{-1}$). Alternate pulses (0.265 mL) of pure O_2 and pure CO were injected every 2 min [24]. The oxygen storage capacity (OSC) was calculated from the CO consumption after stabilization.

3. Results and discussion:

3.1. BET and XRD

Table 2 shows the BET surface area of the catalysts after the different treatments. The stabilized ceria-zirconia supported catalysts exhibit similar areas, between 61 and 63 $m^2.g^{-1}$. The reduction and the aging treatments induce a small decrease of 5-10% and 5-8%, respectively. The zirconia-rich sample is the more stable ceria-zirconia sample toward reduction, and the less stable toward aging. The sulfating treatment is a little more severe, with a loss between 13% and 18%. After aging and consecutive sulfating treatment, the decrease of the surface area is more significant, until 36-38% for Pt/Ce70 and Pt/Ce58. Representative diffractogramms, obtained with Pt/Ce70, are reported Figure 1. The XRD data of the Pt/CeX catalysts are in agreement with the BET measurements. Whatever the treatment, the width of the main peak, which is related to the mean particle size, is rather constant for the ceria-zirconia based catalysts, except after sulfating and aging. A small decrease is then observed. The average particle size deduced from the Scherrer equation are 7.6 nm, 8.2 nm and 9.3 nm for the stabilized, the reduced, and the sulfated and consecutively aged Pt/Ce70 catalysts, respectively. In the latter case, in addition to the sintering, a pore filing by sulfates can occur, in accordance with the decrease of the surface areas of the sulfated samples.

Concerning the pure ceria supported sample, a high surface area is observed after stabilization, at 94 $m^2.g^{-1}$ (Table 2). However, this catalyst is more sensitive to the different treatments than the ceria-zirconia supported samples. The sulfating treatment leads to a loss of 34% of the initial surface area, and a dramatically collapse is observed after the reduction treatment (-80%). The XRD patterns of the stabilized and reduced Pt/Ce100 samples (Figure 1) are in accordance with these results. The mean particle size greatly increases after the reducing treatment, from 8.8 nm to 20.3 nm using the Scherrer equation. The oxidizing treatment at 800°C also leads to a severe sintering (-55% for the surface area), and a sulfating and consecutive aging treatment induces a stronger decrease of the surface area, at only 18 $m^2.g^{-1}$ (Table 2).

With all these catalysts, note that there is no supplementary surface loss after the desulfating treatment, a small recovery of few $m^2.g^{-1}$ can be observed (not reported in Table 2), which is in agreement with a pore filling by sulfates.

The Pt/Ba/Al catalyst surface area is not affected by these different treatments, at around 118 m^2g^{-1}. However, it has been previously established with this catalyst [5] that aging at 800°C favors the barium aluminates formation while aging after sulfating leads to bulk barium sulfate formation.

Table 2: BET surface areas ($m^2.g^{-1}$) of the studied catalysts.

	BET surface areas ($m^2.g^{-1}$)				
Catalyst	Stabilized (700°C)	Reduced (700°C)	Sulfated	Aged (800°C)	Sulfated and aged
Pt/Ce100	94	18	62	42	18
Pt/Ce70	61	55	52	57	38
Pt/Ce58	62	55	51	59	40
Pt/Ce20	63	60	55	58	49
Pt/Ba/Al	118	-	118	119	117

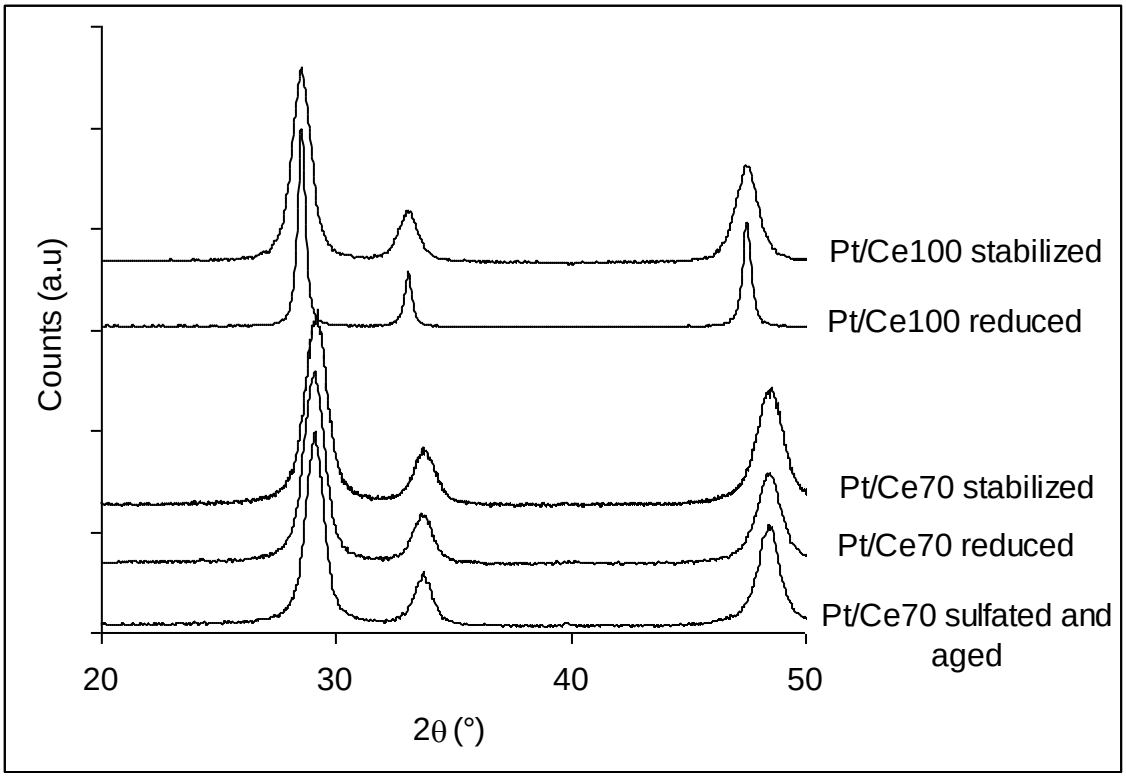

Figure 1: X ray diffractogramms of Pt/Ce70 and Pt/Ce100 after stabilization, after reduction (R700) and after sulfating and aging (+S+A800).

3.2. NOx storage capacity and TPR measurements

3.2.1. Stabilized catalysts

The NOx storage capacities (NSC) of the stabilized catalysts were measured at 200, 300 and 400°C in lean mixture containing H_2O and CO_2. The results for a storage time of 100s are reported in Table 3.

The Pt/Ba/Al catalyst exhibits NSC between 13.1 $\mu mol.g^{-1}$ at 200°C and 18.3 $\mu mol.g^{-1}$ at 400°C. These results were discussed in detail in a previous study [23] and were attributed to relatively strong surface basicity. It allows a higher NSC at high temperature due to a good nitrate thermal stability, but it also induces competition with H_2O and especially CO_2. Same evolution with temperature is obtained with Pt/Ce100, which indicates the presence of relatively strong basic sites too. Some changes occur with the ceria-zirconia supported samples. The NSC of Pt/Ce70 is nearly constant with the temperature test, and the optimal temperature is observed at 200°C for Pt/Ce58 and Pt/Ce20. Then, the optimal storage temperature decreases with the increase of the Zr content. Therefore, the increase of the zirconia content induces a weaker basicity. The NO oxidation activity, expressed as the NO_2/NOx ratio at saturation is reported in Figure 2. No correlation was observed between the NSC and the NO oxidation activity. Actually, the influence of the support composition is rather limited but the NO_2/NOx ratio strongly increases with the temperature test. It is very low at 200°C, generally below 10%, and increases near 30% at 400°C (Figure 2).

Compared to Pt/Ba/Al, the higher NSC of Pt/Ce100 can be attributed to the fact that the entire support surface may participate to the NOx storage, whereas it occurs mainly on the Ba surface on Pt/Ba/Al. The NSC of the ceria-zirconia supported catalysts are a little lower than with Pt/Ce100, but their specific areas are 30% lower. In order to observe if a correlation exists between the NSC behavior and the redox properties, the samples characterized by H_2-TPR.

Table 3: NOx storage capacities calculated for the first 100 seconds ($\mu mol.g^{-1}$)*. Influence of the temperature test and the catalyst treatment (stabilized or reduced catalysts).

Catalyst	NOx storage capacity ($\mu mol.g^{-1}$) stabilized catalysts			NOx storage capacity ($\mu mol.g^{-1}$) reduced catalysts R700		
temperature	200°C	300°C	400°C	200°C	300°C	400°C
Pt/Ce100	20.9	22.8	24.2	8.7	14.0	9.6
Pt/Ce70	17.1	16.9	16.7	19.4	23.1	21.3
Pt/Ce58	23.0	17.4	15.5	23.2	24.9	19.8
Pt/Ce20	18.1	16.0	12.8	19.3	21.1	16.6
Pt/Ba/Al	13.1	13.8	18.3			

* 67 $\mu mol.g^{-1}$ are injected in 100s

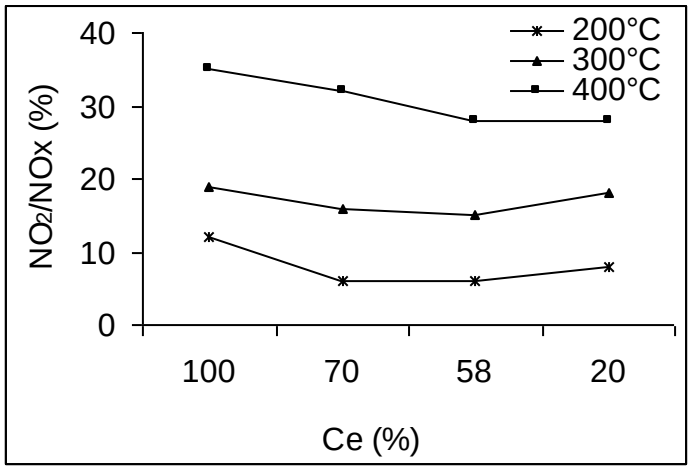

Figure 2: NOx storage test: NO_2/NOx ratio at saturation (stabilized catalysts) depending on the ceria-zirconia support composition.

The TPR profiles of the Pt/CeX catalysts are reported in Figure 3. A main reduction peak is observed in the 120-300°C temperature range, depending on the material composition. It corresponds to the easily reducible Ce^{IV} reduction in Ce^{III}. The higher the zirconium content is, the lower the temperature peak is (maxima between 180 and 260°C). The corresponding H_2 consumptions ($\mu mol.g^{-1}$) are plotted in Figure 4A. The Pt/Ce58 and Pt/Ce70 catalysts exhibit the highest reducibility. Nevertheless, there is no direct correlation between this parameter, which is linked to the oxygen mobility and would influence the NO oxidation, and the NOx storage capacity.
However, ceria containing catalysts are known for their redox properties. Then, a reducing pre-treatment may modify the NOx storage behaviors.

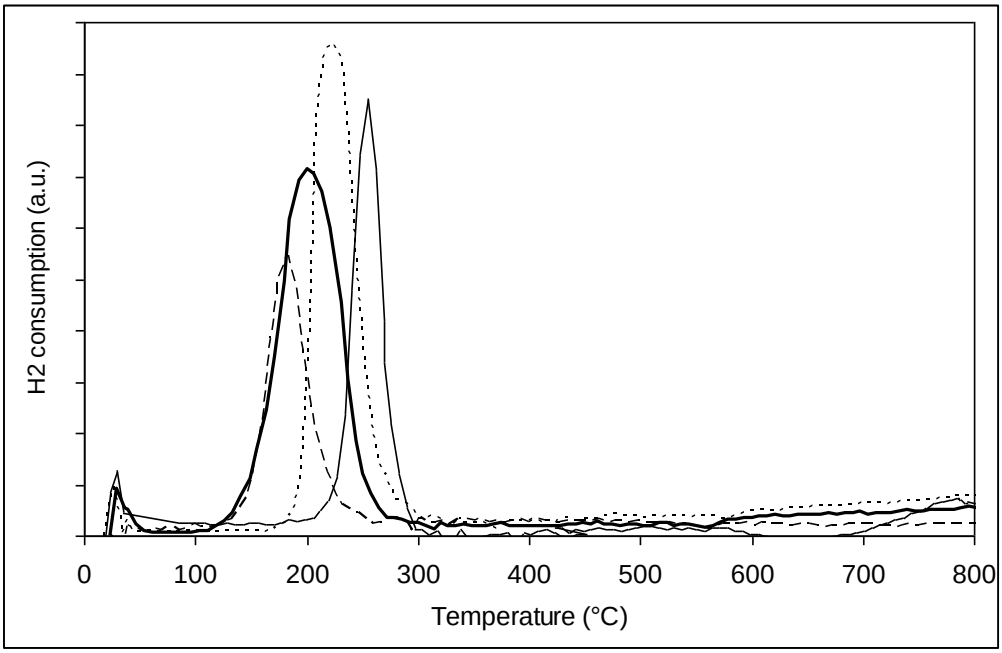

Figure 3: TPR profiles of the Pt/CeX stabilized catalysts: Pt/Ce100 (—), Pt/Ce70 (···), Pt/Ce58 (**—**) and Pt/Ce20 (---).

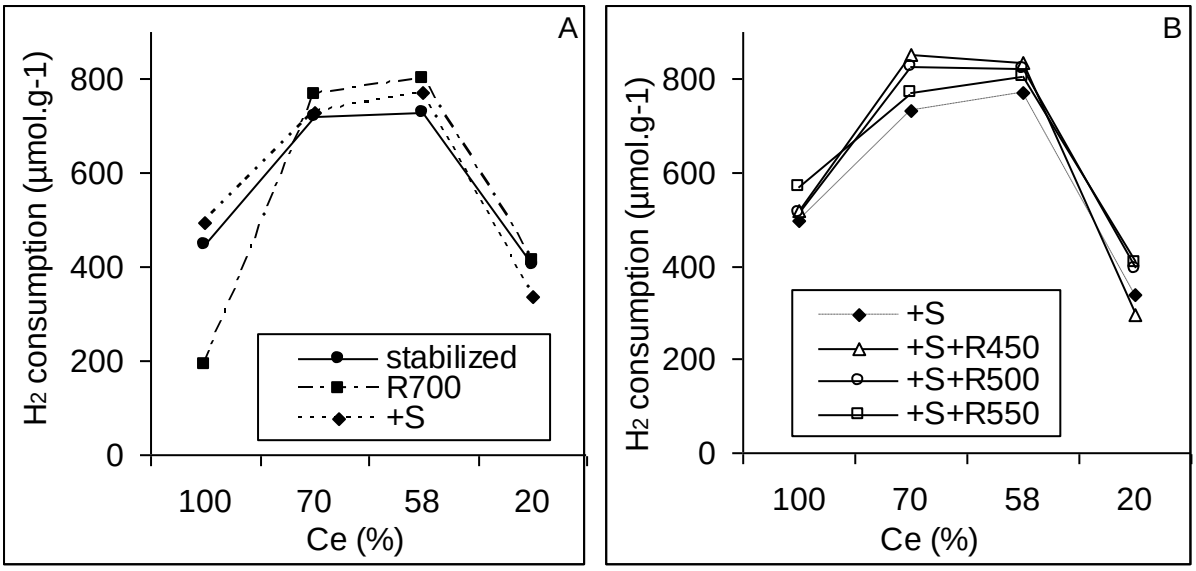

Figure 4: H_2 consumptions (µmol.g^{-1}) corresponding to the "easily" reducible Ce^{IV} of the Pt/CeX catalysts deduced from the TPR measurements (100°C<Tr<350°C). A) stabilized catalyst (•), reduced catalyst R700 (■), sulfated catalyst +S (♦) ; B) sulfated catalyst +S(♦), after regeneration at 450°C (△), after regeneration at 450°C (○), after regeneration at 450°C (□).

3.2.2. Reduced catalysts (R700)

The NOx storage capacities of the reduced ceria-zirconia supported catalysts are reported in Table 3. Compared with the stabilized samples, the NOx storage capacities are nearly unchanged at 200°C but raise at 300 and 400°C with a mean increase of 37% and 28%, respectively. Then, the optimal storage temperature is shifted from 200°C (stabilized catalysts) up to 300°C (reduced catalysts), which would mean that the reducing treatment induces a small increase of the catalysts basicity.

At 300°C, the NOx storage capacities of the ceria-zirconia supported catalysts reach values between 21.1 and 24.9 µmol.g^{-1}. On the contrary, the Pt/Ce100 sample exhibits a strong decrease of the NOx storage capacity (-40%) after reduction which is attributed to the dramatic decrease of the surface area (Table 2).

This NOx storage improvement after the reducing treatment can be attributed to higher oxidation properties since the NO oxidation activity also increases. Indeed, the NO_2/NOx ratio (%) at saturation, reported in Table 4 for the tests at 300°C, significantly increases on the R700 samples, especially for the high cerium loading compositions. For instance, it increases from 15-16% to 32-35 % for the Pt/Ce58 and Pt/Ce70 catalysts.

Table 4: Influence of the reduction treatment on the NO oxidation activity at 300°C, expressed as the NO_2/NOx (%) ratio after saturation.

	NO_2/NOx (%) at saturation				
	Stabilized catalyst	R700	Sulfated	Sulfated and aged	+S+R550
Pt/Ce100	19	29	20	11	25
Pt/Ce70	16	32	18	11	20
Pt/Ce58	17	35	16	13	29
Pt/Ce20	18	20	18	16	21

The platinum state should not play an important role for these changes since it may be not so different during the test, depending on the different treatments. On alumina (Pt/Ba/Al), bulk platinum is reduced even after the stabilization treatment at 700°C in oxidizing atmosphere. Corresponding Pt X-ray diffraction peak is easily detectable [23]. Platinum is known to be better dispersed/stabilized on CeZr materials due to strong Pt-O-Ce link [25] and neither Pt nor PtO XRD peaks are detected (Figure 1). Moreover, before the NOx storage capacity measurement (as before the NOx conversion test in cycling conditions), the catalysts were pretreated *in situ* for 30 min at 550°C, under a 10% O_2, 10% H_2O, 10% CO_2 and N_2 mixture (section 2). Then, whatever the previous treatment, we can assume that platinum should be metallic with a partially oxidized surface for alumina supported catalysts, and probably in a little more oxidized state on ceria-zirconia. Finally, the reducing pretreatment should not lead to very different platinum states for the storage test. Beside, in 2004, Perrichon et al. [26] studied the metal dispersion of CeO_2–ZrO_2 supported platinum catalysts measured by H_2 or CO chemisorption. It was demonstrated that the platinum dispersion was nearly constant for a wide range of composition of the mixed oxide between $Ce_{0.15}Zr_{0.85}$ and $Ce_{0.68}Zr_{0.32}$.

To explain the evolutions observed after the reducing treatment, the redox behavior of the reduced samples was investigated by both H_2-TPR measurements and oxygen storage capacity (OSC) tests.

After the usual oxidation pretreatment (section 2.4), the TPR profiles of the reduced samples show a shift of the main reduction peak to lower temperature (Figure 5). The H_2 consumption starts at room temperature and the reduction of the easily reducible Ce^{IV} is finished near 150°C. This improvement of the cerium reducibility in ceria-zirconia materials after a reducing treatment is well known [27,28]. It can be attributed to a structural re-organization of ceria-zirconia, and to the reduction of the platinum particles, according to Fan et al. [29].Compared to the stabilized catalysts, there is no significant change of the H_2 consumption related to the easily reducible Ce^{IV}, except for the Pt/Ce100 catalyst because of the surface area loss (Figure 4A).

To complete this study, the oxygen storage capacities of the reduced samples were measured at 200, 300 and 400°C with the CO-pulsed method and the results (Table 5) were compared with the NO_2/NOx ratio measured at the same temperatures at the end of the storage test. The results

are reported in Figure 6 and they clearly show a correlation between the oxygen storage capacity, which is linked to the oxygen mobility, and the NO oxidation activity. Note that the better result for each temperature depends on the support composition. The low cerium loading catalyst Pt/Ce20 is the more active at low temperature, whereas the best results are obtained with the cerium-rich samples at higher temperature.

Finally, compared to the stabilized samples, the reduced ceria-zirconia supported catalysts exhibit higher NOx storage capacities which can be attributed to an enhancement of the redox behaviors. Particularly, the NO oxidation reaction, which is the first step of the storage process, is largely improved. However, the NO oxidation rate is not the only limiting parameter in this study. Indeed, Pt/Ce20 and Pt/Ce70 catalysts, which exhibit similar surface areas and different redox behaviors, have similar NOx storage properties.

Table 5: Oxygen storage capacities (OSC) ($\mu mol_O.g^{-1}$) measured with the CO-pulsed method at 200, 300 and 400°C. Influence of the catalyst treatment.

	stabilized			reduced			sulfated		
Temp.	200°C	300°C	400°C	200°C	300°C	400°C	200°C	300°C	400°C
Pt/Ce100	116	185	227	20	36	69	24	46	142
Pt/Ce70	117	488	716	80	327	667	42	238	671
Pt/Ce58	164	554	752	112	438	638	49	273	663
Pt/Ce20	103	248	362	96	243	417	20	94	279

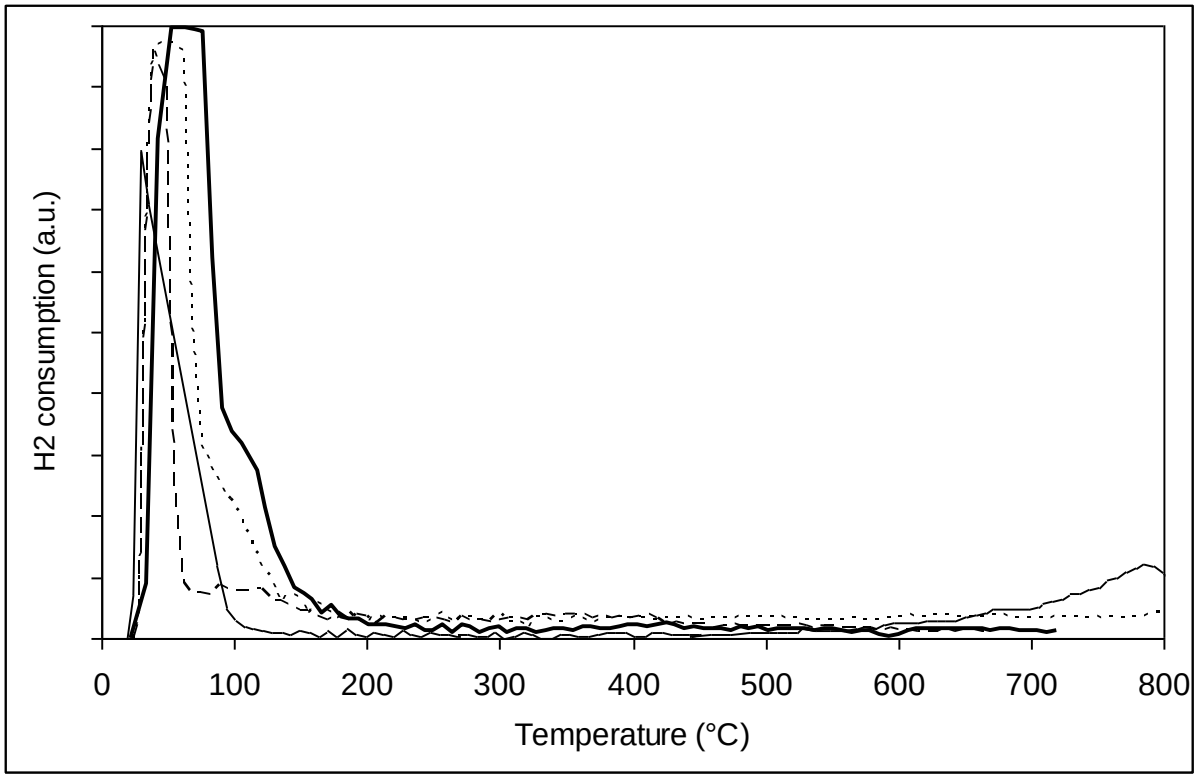

Figure 5: TPR profiles of the reduced (R700) Pt/CeX catalysts: Pt/Ce100 (—), Pt/Ce70 (···), Pt/Ce58 (**—**) and Pt/Ce20 (---)

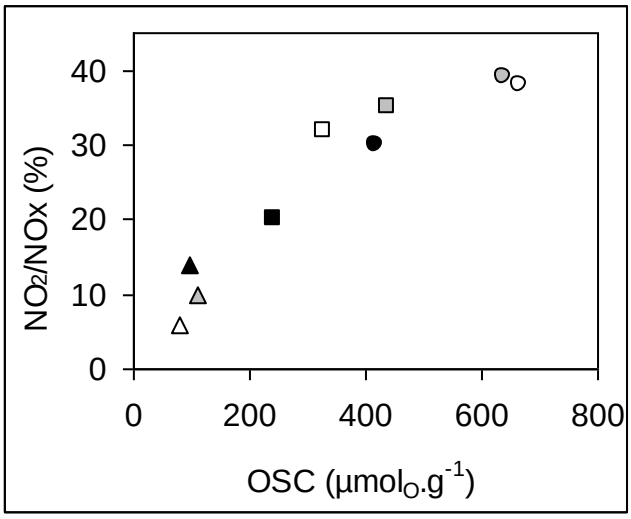

Figure 6: Reduced (R700) catalysts: relationship between the NO oxidation activity, express as the NO_2/NOx (%) ratio at saturation, and the OSC ($\mu mol_O.g^{-1}$). Temperature tests: 200°C (triangle), 300°C (point) and 400°C (square) for Pt/Ce20 (black symbol), Pt/Ce58 (grey symbol) and Pt/Ce70 (blank symbol).

3.2.3. Sulfated catalysts, aging and regeneration

3.2.3.1. Sulfated catalysts.

Only the stabilized catalysts were submitted to sulfur poisoning, aging and regeneration. After the different treatments, the NOx storage capacities were measured only at 300°C with H_2O and CO_2 in the feed stream. The corresponding results are reported in Table 6.

Table 6: NOx storage capacities ($\mu mol.g^{-1}$) at 300°C depending on the catalyst treatment (calculated for the first 100 seconds).

Catalysts	Pt/Ce100	Pt/Ce70	Pt/Ce58	Pt/Ce20	Pt/Ba/Al
Stabilized sample (700°C)	22.8	16.9	17.4	16.0	13.8
Reduced sample (R700)	14.0	23.1	24.9	21.1	-
Sulfated sample (+S)	8.3	5.3	3.6	3.3	4.6
+S +A800	3.6	*6.5*	7.4	7.9	11.1
+S+R450	5.2	9.8	9.4	8.0	
+S+R500	20.1	21.0	19.6	16.7	11.9
+S+R550	19.6	19.7	19.1	16.4	15.6
+S+A800+R500		12.0			
+S+A800+R550		17.1			12.0

The sulfated catalysts show a dramatic decrease of their NOx storage capacities. The sulfated Pt/CeX catalysts exhibit very low NOx storage properties, between 3.3 and 8.3 $\mu mol.g^{-1}$, with a negative impact of the Zr content. The average storage loss is between 64% (Pt/Ce100) and 80% (Pt/Ce58 and Pt/Ce20). The Pt/Ba/Al catalyst is also very affected by the sulfur poisoning, with a loss of 66%. Note that the Pt/Ba/Al BET surface area is not affected by the sulfating treatment whereas Pt/Ce100 and Pt/CeZr catalysts have lost 34% and around 10%, respectively.
The sulfated catalysts were then characterized by H_2-TPR. The reduction profile of the sulfated Pt/Ba/Al catalyst (not shown but already reported in ref [30] for example) exhibits three main reduction peaks in the 400-800°C temperature range, all related with sulfates reduction. They were ascribed to (i) simultaneous reduction of aluminum sulfates and well dispersed barium sulfates located in platinum proximity, (ii) surface barium sulfates reduction and (iii) bulk sulfates reduction.
The TPR profiles of the sulfated Pt/CeX samples are reported in Figure 7. Compared to the stabilized ones (Figure 3), the sulfating treatment leads to both a broadening of the low temperature peak (Ce^{IV} reduction) and the appearance of an important hydrogen consumption

between 300-350°C and 600°C. Even if the sulfur poisoning does not significantly modify the amount of easily reducible Ce^{IV} (Figure 4), the OSC measurements (Table 5) indicate a strong decrease of the oxygen mobility, especially at low temperature and for the higher Zr content. For the ceria-zirconia supported catalysts, the mean losses are 70%, 55% and 15% at 200°C, 300°C and 400°C, respectively. The effect on Pt/Ce100 is even more pronounced, with an OSC loss of 80%, 75% and 40%, respectively. Then, the sulfur poisoning seems to induce a limitation of the oxygen mobility mainly at the surface level. However, the NO oxidation activity at 300°C is nearly not affected by the sulfating treatment (Table 4). This result is rather in accordance with support reducibility deduced from the TPR experiments.

The hydrogen consumption observed at high temperature (T_r > 300-350°C) corresponds to the reduction of surface and bulk sulfates formed on ceria–zirconia support [31]. In addition, Figure 7 shows that the higher the zirconium content is, the higher the temperature of the end of the sulfate reduction is. It varies between 550°C for Pt/Ce100 and 610°C for Pt/Ce20. This latest sample also exhibits the broader sulfate reduction temperature range since it occurs from 350°C. However, all these Pt/CeX catalysts exhibit a sulfate reduction achievement at significant lower temperatures than Pt/Ba/Al [30], the improvement being between 190°C and 250°C.

The integration of the H_2 consumption corresponding to the sulfate reduction allows the evaluation of the sulphur content (Table 7), assuming a H_2/SO_4^{2-} ratio of 4 for the sulfate reduction ($X\text{-}SO_4 + 4H_2 \rightarrow X\text{-}S + 4H_2O$ and/or $X\text{-}SO_4 + 4H_2 \rightarrow X\text{-}O + H_2S + 3H_2O$,). For the Pt/CeX catalysts, the amount of sulfur injected in the gas flow during the sulfating treatment (2 wt %) is not totally deposited. It varies with the increase of the Zr content, from 1.24% for PtCe100 to 1.41% for Pt/Ce20. For comparison, the sulfur content on the Pt/Ba/Al catalyst reaches 1.56%. These sulfur rates are consistent with results obtained by the pyrolysis technique

Table 7: Sulfur content (wt %) and sulfur elimination rate (%, between bracket) deduced from the TPR experiments, depending on the applied treatments. Sulfated sample (+S), sulfated and aged sample at 800°C (+S+A800); sulfated and regenerated sample at 450°C (+S+R450), 550°C (+S+R500) and 550°C (+S+R500), sulfated, aged and regenerated sample (+S+A800+R550)

Catalysts	Pt/Ce100	Pt/Ce70	Pt/Ce58	Pt/Ce20	Pt/Ba/Al
+S	1.24	1.26	1.32	1.41	1.56
+S+A800	0.10	0.19	0.21	0.22	1.42
(sulfur elimination rate (%))	(92%)	(85%)	(84%)	(84%)	(9%)
+S+R450	0.22	0.50	0.51	0.46	-
(sulfur elimination rate (%))	(82%)	(60%)	(62%)	(68%)	-
+S+R500	0.15	0.15	0.11	0.05	0.76
(sulfur elimination rate (%))	(88%)	(88%)	(92%)	(96%)	(51%)
+S+R550	0.11	0.09	0.07	0.01	0.69
(sulfur elimination rate (%))	(91%)	(93%)	(95%)	(99%)	(56%)
+S+A800+R550		≈0			1.37
(sulfur elimination rate (%))	-	(100%)	-	-	(12%)

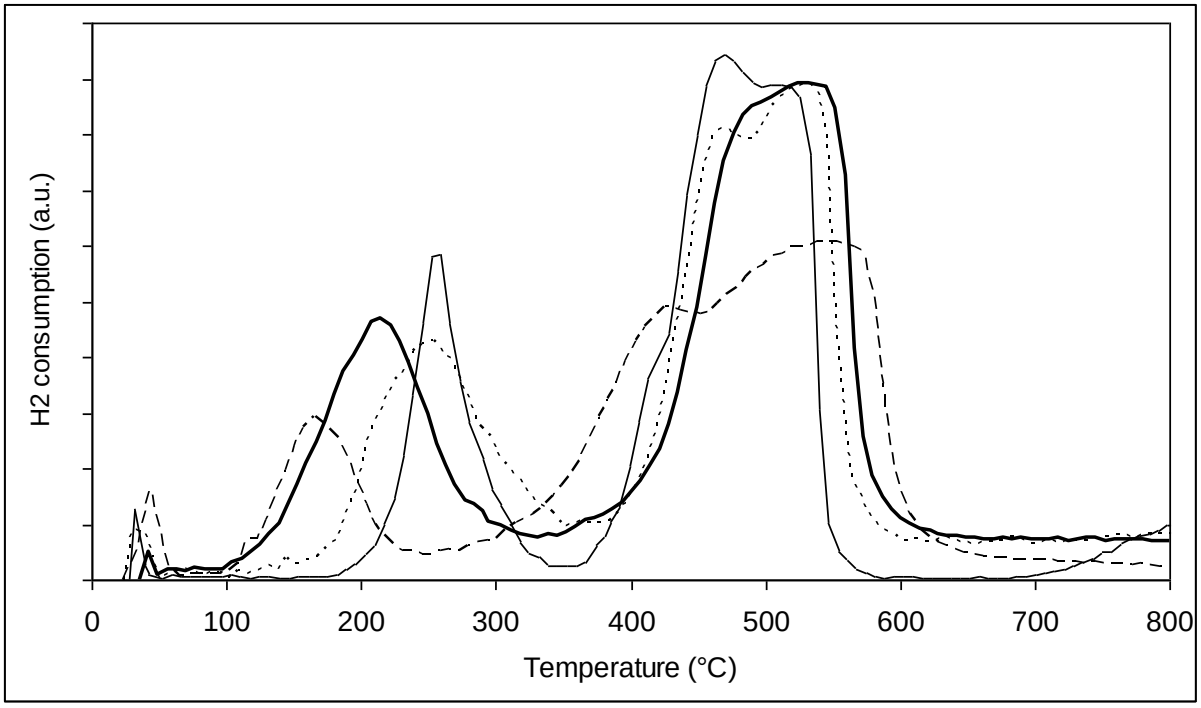

Figure 7: TPR profiles of the sulfated Pt/CeX catalysts: Pt/Ce100 (—), Pt/Ce70 (···), Pt/Ce58 (**—**) and Pt/Ce20 (---).

3.2.3.2. Thermal aging of the sulfated catalysts

The aging at 800°C of the sulfated ceria-zirconia supported catalysts leads to a small recovery of the NOx storage capacity at 300°C (Table 6), even though the specific surface area show a significant decrease, near 20% (Table 2). On the contrary, the Pt/Ce100 catalyst decreases again, which can be attributed to the strong surface area loss compared to the sulfated sample (-70%). Compared to the stabilized samples, the NO oxidation rate of the Pt/CeX catalysts, expressed as the NO_2/NOx ratio at saturation, is lower (Table 4), which can be attributed to a platinum sintering. In the same time, nearly 85% of the deposited sulfur is eliminated by the aging treatment at 800°C on the ceria-zirconia catalysts, only 0.19-0.22% S remains (Table 7). The sulfur elimination reaches 92% on Pt/Ce100, 0.10% S remains.

The sulfated Pt/Ba/Al catalyst is also favorably affected by the aging treatment at 800°C. Its surface area is unchanged and a partial recovery of the NOx storage capacity is obtained (80% of the initial value is restored). After the aging treatment, its NOx storage capacity is significantly higher than the Pt/CeX catalysts. However, the sulfur elimination due to the aging treatment is very small: 9% (Table 7), indicating that only the surface is cleaned.

3.2.3.3. Sulfates stability in reducing atmosphere.

It was previously observed for Pt/Ba /Al samples that a sulfated catalyst reduced at 800°C under 1% H_2/Ar (TPR protocol) and reoxidized at 400°C still exhibits a H_2 consumption corresponding to sulfates reduction during the consecutive TPR. Indeed, during the first TPR run, a part of the sulfates can be reduced in sulfide [5]. Then, the stored sulfur was only partially eliminated, even though all sulfates were reduced at the end of the test, i.e. at 800°C. Then, similar experiments were carried out on the Pt/CeX samples. Representative results, obtained

with the Pt/Ce20 catalyst, are plotted in Figure 8. This graph clearly shows that a part of the sulfur is not eliminated after the first TPR treatment, event if the sulfate reduction is achieved. Around 0.36 wt% S remains, probably as sulfides, compared to 1.41 wt% initially. A weak stabilization of the re-formed sulfates is observed, but the reduction is achieved at 600°C. It can be also observed that the first reduction treatment of the sulfated sample induces the same Ce^{IV} reduction improvement as previously observed for the un-sulfated Pt/CeX samples. After a first reduction, the H_2 consumption corresponding to the easily reducible Ce^{IV} is shifted to lower temperature with a maximum at 50°C, without any change of the corresponding H_2 consumption (around to 420 $\mu mol_{H2}.g^{-1}$).

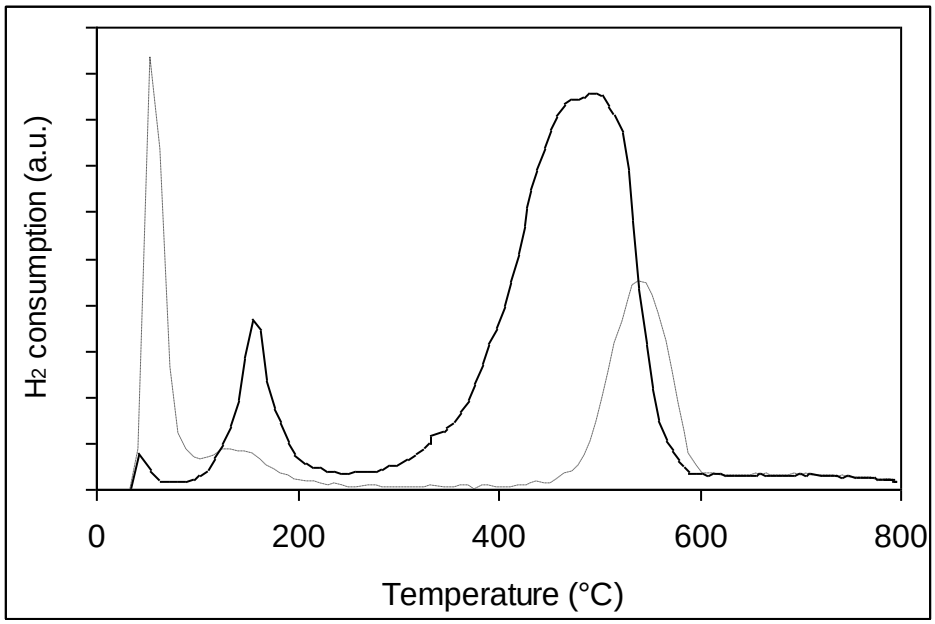

Figure 8: TPR profiles of Pt/Ce20 + S (—) and Pt/Ce20 + S after the first TPR until 800°C and reoxidized at 300°C (---).

To improve the sulfur elimination, a reducing treatment with a mixture containing 2.5% H_2, 10% CO_2, 10% H_2O and N_2 was found to be appropriate [5]. The optimum regeneration temperature depends on the catalyst composition, with a compromise between the sulfur elimination rate and the possible thermal aging. For instance, for a 0.5h treatment, 650°C was found to be optimal for a Pt/20wt%BaO/Al_2O_3 catalyst [5] and 550°C is enough for Pt/10wt%BaO/Al_2O_3 or Pt/10wt%BaO/$Ce_{0.7}Zr_{0.3}O_2$ [19]. In this study, three regeneration temperatures were tested: 550°C, 500°C and 450°C.

After regeneration at 550°C, from 90% to 99% of the initially deposited sulfur on the Pt/CeX catalysts is removed (Table 7). The elimination rate increases with the zirconium content. This elimination rate is still very high after a regeneration treatment at 500°C, between 88% and 96%. However, it decreases to 60%-68% at 450°C for the ceria-zirconia supported catalysts, whereas the sulfur elimination reaches 82% for Pt/Ce100. The corresponding TPR characterizations are presented in Figure 9 for Pt/Ce100 and Pt/Ce20.

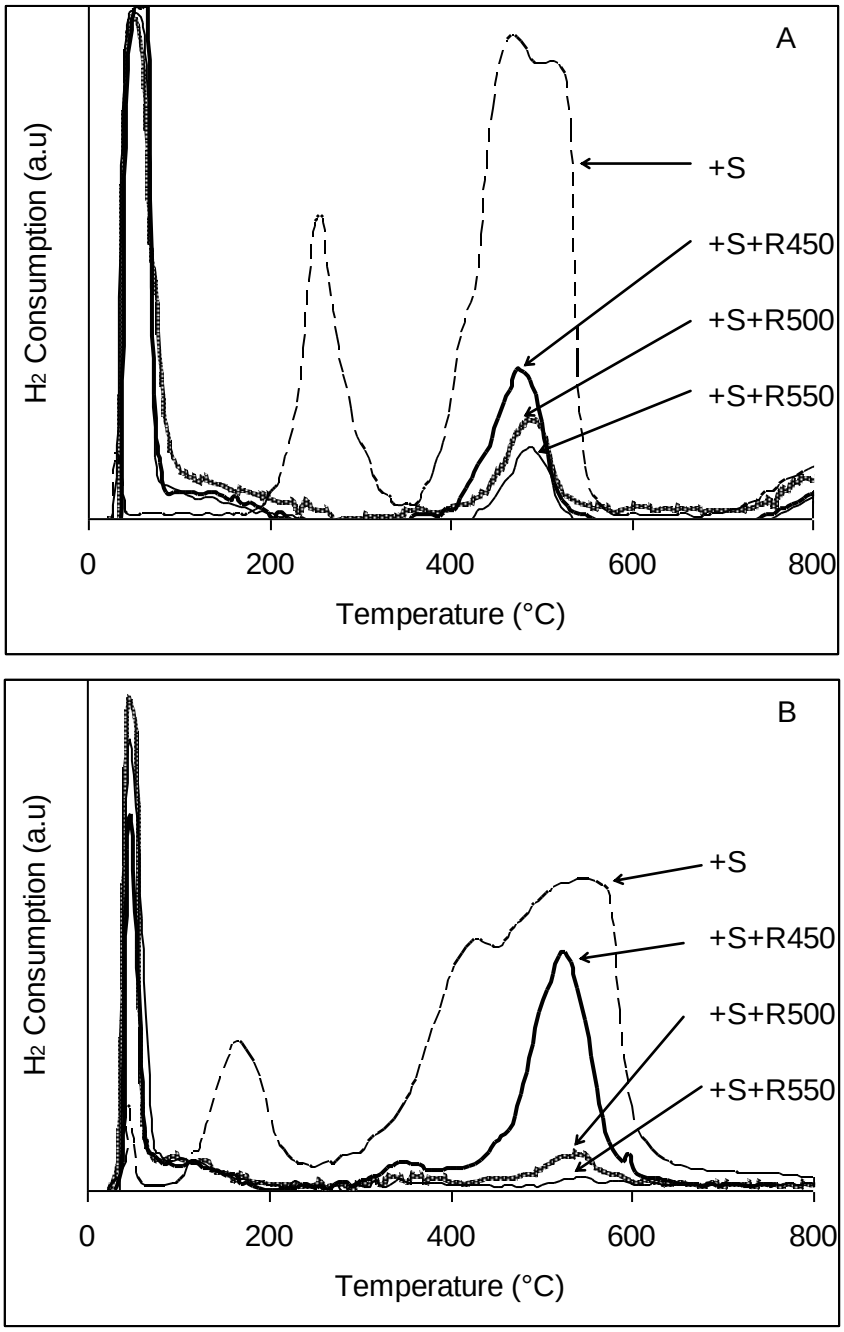

Figure 9: TPR profiles of A) Pt/Ce100 and B) Pt/Ce20. Sulfated sample (--), after regeneration at 450°C +S+R450 (—), after regeneration at 500°C +S+R500 (▪▪▪), after regeneration at 450°C +S+R550 (—).

Compared to the Pt/CeX catalysts, the sulfur elimination on Pt/Ba/Al is significantly lower. Only half of the initial deposited sulfur is removed at 500°C, and the rate increases to only 56% at 550°C (Table 7).

Compared to the stabilized catalysts, the NOx storage capacity at 300°C is at least fully recovered after the regeneration treatment at 550°C for all the catalysts, except Pt/Ce100 (Table 6). The slight improvements on the ceria-zirconia supported catalysts can be attributed to the reducing treatment, as seen previously for the reduced samples (R700). Indeed, Figure 9 shows

that the improvement of the cerium reducibility is also obtained after the regeneration treatment in lean atmosphere and data reported Table 4 show that the NO_2/NOx ratio is improved too. The influence of a reducing treatment can also explain the Pt/Ce100 decline since the surface area of this sample is very sensitive to sintering under reducing atmosphere (Table 2). The decrease of the regeneration temperature down to 500°C leads to similar results for Pt/CeX catalysts (Table 6). On the contrary, this temperature is not sufficient for Pt/Ba/Al, only 86% of the initial NOx storage capacity is recovered. For Pt/CeX catalysts, it was then interesting to test lower regeneration temperature: 450°C for 0.5h. Measurements show that this condition is not severe enough to totally restore the initial NOx storage capacities. Near half of the initial capacities were then obtained for ceria-zirconia supported samples.

Some additional tests were performed with Pt/Ba/Al and Pt/Ce70 (selected as Pt/CeX sample) to evaluate the regeneration of sulfated and consecutively aged samples (+S+A800). After regeneration at 550°C, the sulfated and aged Pt/Ba/Al catalyst exhibits a good recovery of the NOx storage capacity, at 12µmol.g^{-1}, i.e. 87% of the initial value (Table 6). However, the aging treatment also induces a stabilization of the sulfates since only 12% of the initial deposited sulfur is eliminated, whereas 9% was already eliminated after aging (Table 7). On the contrary, the sulfates are fully eliminated on the Pt/Ce70 catalyst after aging and regeneration at 550°C or 500°C. If the NOx storage capacity is not fully recovered after regeneration at 500°C, reducing treatment at 550°C leads to a total regeneration (Table 6).

3.3. NOx conversion in cycling conditions

The NOx removal efficiency was measured in cycling rich/lean condition. Since a reducing treatment influenced the NOx storage properties of the ceria-zirconia supported catalysts, only the pre-reduced samples was studied. For comparison, the Pt/Ba/Al catalyst was also tested. Whatever the used conditions and catalyst, no significant amount of N_2O was observed. Typical recorded curves, obtained with Pt/Ba/Al at 400°C, are presented Figure 10. The results obtained with 3% H_2 in the rich periods are reported in Figure 11A.

At 200°C, the Pt/Ba/Al reference catalyst exhibits 66% of NOx removal efficiency. At this temperature, only 34% of the introduced hydrogen reacts. In the same time, the ammonia formation is significant, corresponding to a selectivity of 28%. The increase of the temperature test to 300°C leads to an improvement of the NOx conversion up to 78%. As the NOx storage capacities are similar at 200°C and 300°C for this sample (Table 3), it means that the reducing step is improved, in accordance with the increase of the hydrogen consumption to 41%. However, the ammonia selectivity remains nearly unchanged, at 30%. At 400°C, the NOx conversion does not increase anymore, but both hydrogen consumption and ammonia selectivity increase, at 52% and 36%, respectively.

With Pt/Ba/Al, the hydrogen concentration is not the limiting parameter since less than half of the injected H_2 is converted with 3%H_2 in the rich pulse. Then, as expected, increasing the H_2 concentration to 6% in the rich pulse does not significantly affect the behavior of Pt/Ba/Al (Figure 11B). Re-calculations of the NOx storage capacities during the first 30 s show that around 80%-85% of the inlet NOx is stored. Then, it partially explains the limitation of the NOx conversion. In addition, some NOx desorption can occur without reduction at the beginning of the rich pulses [32,33].

For the ceria-zirconia supported catalyst, the NOx conversions with 3% H_2 in the rich pulses are between 38% and 48% at 200°C and the H_2 consumption rates reach 77%-100%, depending on the support composition (Figure 11A).
Compared to Pt/Ba/Al, these NOx conversion rates are significantly lower even if the NOx storage capacities are quite similar. On the contrary, the H_2 consumption rates are higher (34% for Pt/Ba/Al): a large part of the introduced hydrogen is then consumed by the reduction of the ceria-zirconia supports.
Concerning the ceria-zirconia supported catalysts, the lower conversion rate is obtained with Pt/Ce58, whereas this catalyst exhibits the higher NOx storage capacity (Table 3). Then in this case, the NOx conversion is not directly related with the NOx storage capacity. In the same time, the introduced hydrogen was totally converted for Pt/Ce58 whereas 92% and 77% were consumed with Pt/Ce70 and Pt/Ce20, respectively. These values are related with the kinetics of reduction (OSC) and to the amount of reducible species (TPR). With Pt/Ce58, there is not enough hydrogen to reduce both support and stored NOx. It is important to note that compared with Pt/Ba/Al, the N_2 selectivity is significantly improved with the ceria-zirconia supported catalysts. At 200°C, ammonia formation was observed only with Pt/Ce20, corresponding to 10% selectivity.
Increasing the temperature test to 300°C leads to a significant increase of the NOx removal efficiency at 62-66%, whereas the corresponding NOx storage capacities are nearly the same at 200°C and 300°C. Then, the reducing step was the limiting step at 200°C. Furthermore, the ammonia selectivity at 300°C becomes near nil for all the ceria-zirconia supported catalysts. Note also that the introduced hydrogen is totally converted with Pt/Ce58 and Pt/Ce70, but only 85% with Pt/Ce20 which exhibits the lower OSC.
The increasing of the temperature test to 400°C leads only to a small decrease of the NOx conversion. This can be attributed to the small decrease of the NOx storage capacity at this temperature. Some hydrogen still remains at 400°C with Pt/Ce20, even if its conversion rate increases to 94%.

As the hydrogen consumption can reach 100% with the ceria-zirconia supported catalysts, further investigations were carried out increasing the H_2 concentration in the rich pulse to 6%.
At 200°C, the hydrogen conversion rate reaches 92-93% for Pt/Ce58 and Pt/Ce70 and only 46% for Pt/Ce20 (lower OSC). Comparing with 3% H_2, the NOx conversion rate is just a little improved, and more interestingly, it varies neither with the OSC nor the NOx storage capacity, but with the cerium content (from 47% for Pt/Ce20 to 58% for Pt/Ce70). Simultaneously, the ammonia production decreases with the cerium content, leading to NH_3 selectivity of 16%, 8% and 3% for Pt/Ce20, Pt/Ce58 and Pt/Ce70, respectively.
The increase of the temperature test to 300°C leads to an improvement of the NOx conversion, as well as with 3% H_2. The results are quite similar at 400°C, always with a small improvement with the cerium content. At 300°C and 400°C, at least 90% the hydrogen is converted and the ammonia selectivity tends to become nil for the three ceria-zirconia supported catalysts.

Finally the NOx conversion rate obtained with the ceria-zirconia supported catalysts are lower than those obtained with Pt/Ba/Al. However, the ammonia selectivity is significantly decreased

with the ceria-zirconia mixed oxides. With 3% H_2 in the rich pulse, near no ammonia was observed, excepted with Pt/Ce20 at 200°C (10% NH_3 selectivity). In opposition, the NH_3 selectivity reaches 28%-37% with Pt/Ba/Al, depending on the temperature test.
Whatever the temperature test, with 3% H_2 in the rich pulse, the lower NOx conversion is obtained with Pt/Ce58 and the introduced H_2 is then fully converted. This catalyst also exhibits the higher oxygen mobility/storage capacity.
When 6% H_2 is used in the rich pulse, the NOx conversion rate increases with the cerium concentration in the mixed oxide (relationship neither with the NOx storage capacity nor the OSC). Simultaneously, it also confirms that the ammonia selectivity decreases with the increase of the cerium content, even in case the introduced H_2 is not totally converted.

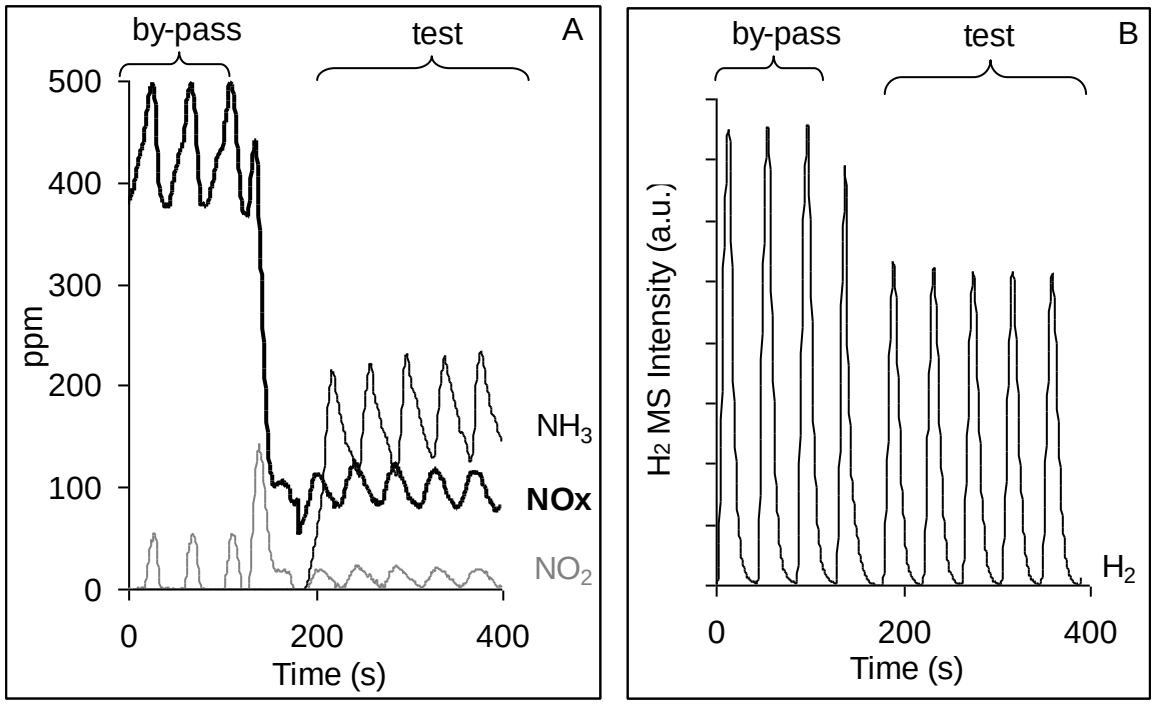

Figure 10: Typical storage-reduction experimental curves. Results obtained at 400°C with stabilized Pt/Ba/Al with 6%H_2 in the rich pulse. A) NOx, NO_2 (chemiluminescence) and NH_3 concentrations (FTIR multigas analyzer), B) H_2 signal (mass spectrometer).

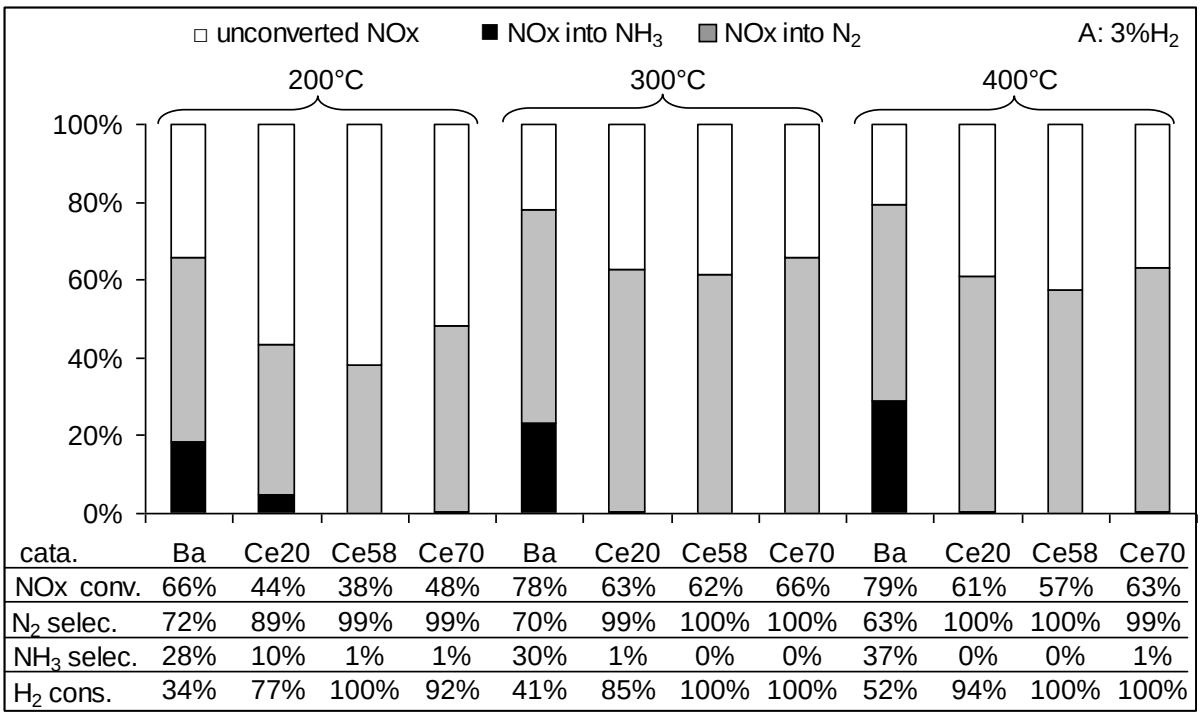

cata.	Ba	Ce20	Ce58	Ce70	Ba	Ce20	Ce58	Ce70	Ba	Ce20	Ce58	Ce70
NOx conv.	66%	44%	38%	48%	78%	63%	62%	66%	79%	61%	57%	63%
N_2 selec.	72%	89%	99%	99%	70%	99%	100%	100%	63%	100%	100%	99%
NH_3 selec.	28%	10%	1%	1%	30%	1%	0%	0%	37%	0%	0%	1%
H_2 cons.	34%	77%	100%	92%	41%	85%	100%	100%	52%	94%	100%	100%

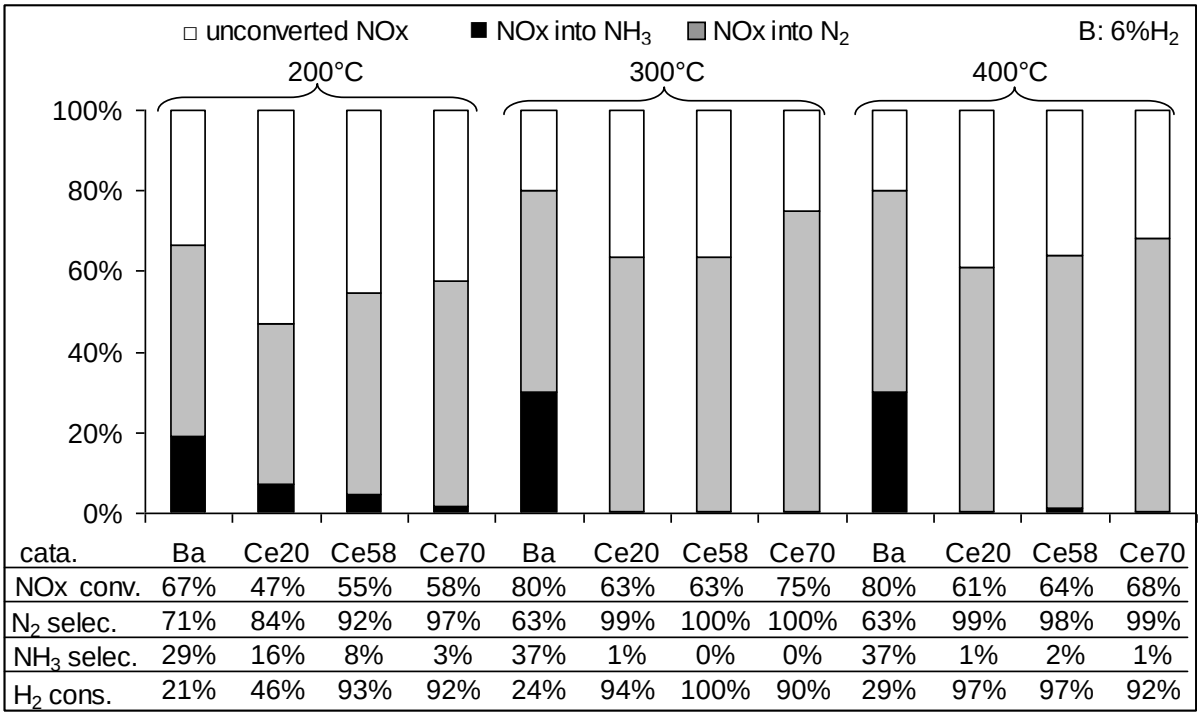

cata.	Ba	Ce20	Ce58	Ce70	Ba	Ce20	Ce58	Ce70	Ba	Ce20	Ce58	Ce70
NOx conv.	67%	47%	55%	58%	80%	63%	63%	75%	80%	61%	64%	68%
N_2 selec.	71%	84%	92%	97%	63%	99%	100%	100%	63%	99%	98%	99%
NH_3 selec.	29%	16%	8%	3%	37%	1%	0%	0%	37%	1%	2%	1%
H_2 cons.	21%	46%	93%	92%	24%	94%	100%	90%	29%	97%	97%	92%

Figure 11: NOx conversion in cycling condition (60s lean, 3s rich). NOx conversion into N_2 (▒), NOx conversion into NH_3 (■), corresponding selectivity and H_2 consumption rate. a) 3%H_2 in the rich pulse; b): 6%H_2 in the rich pulse.
Ba, Ce20, Ce58 and Ce70 are Pt/Ba/Al, Pt/Ce20, Pt/Ce58 and Pt/Ce70, respectively.

4. Conclusion:

The behaviors of the ceria-zirconia supported catalysts are quite similar whatever their composition. Their NOx storage capacities are rather higher than the Pt/Ba/Al model catalyst, with an optimal storage at 200°C versus 400°C for Pt/Ba/Al. The ceria-zirconia supported catalysts are sensitive to a reducing pre-treatment, which leads to an increase of (i) the cerium reducibility/oxygen mobility, (ii) the NO oxidation rate and (iii) the NOx storage capacity at 300 and 400°C. The sulfating treatment leads to a dramatic decrease of the NOx storage capacity for all catalysts, the decrease being more pronounced for the Zr-rich samples. H_2-TPR experiments show that the sulfates amount and their stability tend to increase with the Zr content. However, these sulfates remain significantly less stable compared with Pt/Ba/Al. The sulfur elimination rates in rich mixture at 550°C are higher than 90% with the ceria-zirconia supported catalysts versus 56% with Pt/Ba/Al. The NOx storage capacities are recovered after sulfur regeneration at 500°C only for the ceria-zirconia supported catalysts.

The ceria-zirconia supported catalysts are able to convert NOx in lean-rich cycling condition. Compared with Pt/Ba/Al, the NOx conversions are a little lowered. However, the ammonia selectivity is significantly decreased with the ceria-zirconia mixed oxides. With 3% H_2 in the rich pulses, it reaches 28%-37% with Pt/Ba/Al, depending on the temperature test and, near no ammonia was observed, except with Pt/Ce20 at 200°C (10% NH_3 selectivity). With 6% H_2 in the rich pulses, it was confirmed that the ammonia selectivity decreases with the increase of the cerium content.

Finally, despite a high OSC leading to a reducer over-consumption, the ceria rich sample seems to be the more interesting one. It presents good properties toward NOx storage/sulur regeneration and nearly no NH_3 formation during the NOx conversion in lean-rich cycling condition.

References

[1] W. S. Epling, L. E. Campbell, A. Yezeerets, N. W. Currier, J. E. Parks II, Catal. Rev. 46 (2004) 163.

[2] T. Kobayashi, T. Yamada, K. Kayano, Society of Automotive Engineers, Inc. Technical Papers, 970745

[3] S. Matsumoto, Cattech, Vol.4, no.2, 2000

[4] A. Amberntsson, M. Skoglundh, S. Ljungström, E. Fridell, Journal of Catalysis 217 (2003) 253

[5] S. Elbouazzaoui, E.C. Corbos, X. Courtois, P. Marecot, D. Duprez, Appl. Catal. B 61 (2005) 236

[6] T. Szailer, J.H. Kwak, D.H. Kim, J. Szanyi, C. Wang, C.H.F. Peden, Catal. Today 114 (2006) 86–93

[7] H.Y. Huang, R.Q. Long, R.T. Yang, Appl. Catal. B 33 (2001) 127

[8] K. Yamazaki, T. Suzuki, N. Takahashi, K. Yokota, M. Sugiura, Appl. Catal. B 30 (2001) 459

[9] S. Hodjati, C. Petit, V. Pitchon, A. Kiennemann, Appl. Catal. B 30 (2001) 247

[10] F. Basile, G. Fornasari, A. Grimandi, M. Livi, A. Vaccari, Appl. Catal. B 69 (2006) 58

[11] M. Eberhardt, R. Riedel, U. Göbel, J. Theis, E. S. Lox, Topics Catal. 30/31 (2004) 135.

[12] M. Casapu, J.D. Grunwaldt, M. Maciejewski, M. Wittrock, U. Gobel, A. Baiker, Appl. Catal. B 63 (2006) 232
[13] L. F. Liotta, A. Macaluso, G. E. Arena, M. Livi, G. Centi, G. Deganello, Catal. Today 75 (2002) 439.
[14] .H. Kwak, D.H. Kim, J. Szanyi, C.H.F. Peden, Appl. Catal. B 84 (2008) 545–551
[15] S. Philipp, A. Drochner, J. Kunert, H. Vogel, J. Theis, E. S. Lox, Topics Catal. 30/31 (2004) 235.
[16] P. Svedberg, E. Jobson, S. Erkfeldt, B. Andersson, M. Larsson, M. Skoglundh, Topics Catal. 30 (2004) 199
[17] H.Y. Lin, C.J. Wu, Y.W. Chen, C.H. Lee, Ind. Eng. Chem. Res. 45 (2006) 134.
[18] T. Nakatsuji, J. Ruotoistenmäki, V. Komppa, Y. Tanaka, T. Uekusa, Appl. Catal. B 38 (2002) 101.
[19] E.C. Corbos, S. Elbouazzaoui, X. Courtois, N. Bion, P. Marecot, D. Duprez, Topics Catal. 42–43 (2007) 9
[20] M. Machida, D. Kurogi, T. Kijima, Chem. Mater 12 (2000) 3165
[21] H. Mahzoul, L. Limousy, J.F. Brilhac, P. Gilot, J. of Analytical and Applied Pyrolysis 56 (2000) 179
[22] E.C. Corbos, X. Courtois, F. Can, P. Marecot, D. Duprez, Applied Catalysis B: Environmental 84 (2008) 514–523
[23] E.C. Corbos, X. Courtois, N. Bion, P. Marecot, D. Duprez, Appl. Catal. B 76 (2007) 357
[24] S. Kacimi, J. Barbier Jr., R. Taha, D. Duprez, Catal. Lett. 22 (1993) 343
[25] H. Shinjoh, M. Hatanaka, Y. Nagai, T. Tanabe, N. Takahashi, T. Yoshida, Y. Miyake, Top Catal DOI 10.1007/s11244-009-9371-5
[26] V. Perrichon, L. Retailleau, P. Bazin, M. Daturi, J.C. Lavalley, Appl. Catal. A 260 (2004) 1
[27]P. Fornasiero, J. Kašpar, M. Graziani, Appl. Catal. B 22 (1999) L11 ;
[28] F. Fally, V. Perrichon, H. Vidal, J. Kaspar, G. Blanco, J. M. Pintado, S. Bernal, G. Colon, M. Daturi, J.C. Lavalley, Catal. Today 59 (2000) 373
[29] J. Fan, X. Wu, R. Ran, D. Weng Appl. Surf. Sci., 245 (2005) 162
[30] E.C. Corbos, X. Courtois, N. Bion, P. Marecot, D. Duprez, Appl. Catal. B 80 (2008) 62
[31] M.Waqif, P. Bazin, O. Saur, J.C. Lavalley, G. Blanchard, O. Touret, Appl. Catal. B 11 (1997) 193
[32] W.S. Epling, A. Yezerets, N.W. Currier, Appl. Catal. B 74 (2007) 117
[33] P. Koci, F Plat, Jstepanek, M. Kubıcek, M. Marek Catal. Today 137 (2008) 253